Design and verification of the foundations of the Dahej LNG tanks

J. Martí, F. Martínez
Principia, Madrid, Spain

T. Kanekura, D. Takuwa
IHI, Tokyo, Japan

R. Singh
Petronet LNG, Delhi, India

ABSTRACT: The first two tanks for storage of liquefied natural gas (LNG) at Dahej in Gujarat are already in operation, with the next two currently under construction. Each tank, capable for 148,000 m^3, rests on 578 concrete piles. The more demanding loads on the foundation arise from the hydraulic test and the safe shutdown earthquake (SSE). The former consists in filling the tank with water to achieve 25% greater weight than in operation; the latter, based on the code versions prevailing at the time, corresponds to an earthquake with a return period of 10,000 years.

For axial loads, the pile capacity calculations are straight-forward and their results were verified in full scale tests as per IS 2911. For horizontal loads, however, test results cannot be used directly because the pileheads are rigidly fixed to the slab but are free to rotate in a test pile. The approach followed consisted in constructing *p-y* curves to describe pile-soil interaction at each depth, as well as moment-curvature relations to characterise pile bending; this allowed predicting the response under both tests and earthquakes. The experimental verification of the former was used to confirm the latter, which normally cannot be tested directly.

1 Introduction

The first liquefied natural gas (LNG) terminal in India was commissioned in 2004 in Dahej (Gujarat). The terminal, which is currently being expanded, is owned and operated by Petronet LNG Ltd (PLL). The facilities include a jetty for reception and unloading of LNG tankers, storage tanks where the liquid LNG is temporarily kept and a vaporisation plant to return the liquid to gas form for distribution and use. The present paper is primarily concerned with the storage tanks and, more specifically, with their foundations.

The first development phase of the Dahej terminal provided two LNG storage tanks, each with a net capacity of 148,000 m^3, known as T-101 and T-102. The expansion currently under construction adds two more tanks, T-103 and T-104, with identical design to the two existing ones.

The tanks are of the full containment type, which indicates that they are designed to maintain impermeability to both liquid and gas at -168ºC. This type of tanks are actually double tanks, composed of an outer tank and a self-supporting inner tank. The outer tank consists of a pre-stressed concrete cylindrical wall, capped by a reinforced concrete spherical dome and supported on a reinforced concrete slab. The inner tank is an open top cylindrical tank, made of cryogenic 9% Ni steel in order to ensure good ductility at operating temperatures. Thermal insulation is placed between the two tanks.

When the bottom slab rests directly on the ground, heating must be provided to prevent the ground from freezing under the tank. The Dahej tanks are supported on pile foundations, with piles that protrude 2 m above grade; in this situation air can circulate freely between the slab and the ground and there is no longer a need to heat the slab.

2 Geotechnical and geological setting

Physiographically, the area around the site is made of flat to undulating coastal plains, flood pains, deltaic plains and flats. The relief is generally low, gradually sloping towards the Gulf of Khambat. The Narmada and the Dhadar are the two major rivers flowing into the Gulf of Khambat.

The local ground presents deltaic and tidal deposits, with thicknesses of about 2000 m, which overlie hard Tertiary rocks and the Deccan Trap volcanic formations. The supra-tidal deposits are poligonally cracked mud-flats consisting of about 1 m thick dark grey silt, clay and sand. The inter-tidal deposits are younger mud-flats lying between the high and low tide ranges; these comprise dark grayish and blackish clay and silt mud-flat deposits, with abundant salt marshes and mangrove swamps, typically permeable in nature. The sub-tidal deposits are recent mud-flat accumulations along the margins of Gulf of Khambat and the Narmada creek.

The geotechnical investigation was conducted by Fugro India using field and laboratory techniques. Based on this information, Principia developed a design soil profile for the purpose of supporting the seismic calculations. The ground is made of a series of relatively weak layers, roughly horizontal, where sands, silts and clays alternate down to a depth of about 31 m. Below that, very dense sands are found; the piles penetrate at least two pile diameters into this very dense sand layer, thereby bypassing some 20 m of weak clays directly above. The soil profile adopted is shown in Table 1.

Table 1. Soil profile and characteristics

no. (-)	thickness (m)	depth (m)	description (-)	density (kg/m^3)	SPT (-)	v_s (m/s)	v_p (m/s)	G_o (MPa)	ν (-)
1	3	0-3	sand	1900	18	210	437	84	0.35
2	4	3-7	silt	1900	8	200	816	49	0.48
3	3	7-10	sand	2000	34	270	1377	146	0.48
4	21	10-31	clay	2000	42	350	1785	245	0.48
5	>9	31-40	sand	2100	90	450	2295	405	0.48

Three main lineament sets (trending E-W, ENE-WSW to NE-SW and NW-SE to NNW-SSE) were established in the area, which seem to have played a major role in the development of land forms. The Narmada occupies an ENE-WSW lineament. Most of the lineaments are faults that have divided the area into a number of tectonic blocks.

The geology of the region is described in Figure 1. During the Mesozoic vast areas of western India were covered by lava flows identified as Deccan flood basalt. The state of Maharashtra is mostly covered by the basaltic lava flows of the Deccan Trap. The lava flows extend into the neighbouring states of Madhya Pradesh and Gujarat. The traps have a thickness of 2000 m near the western edge and thin out towards the east.

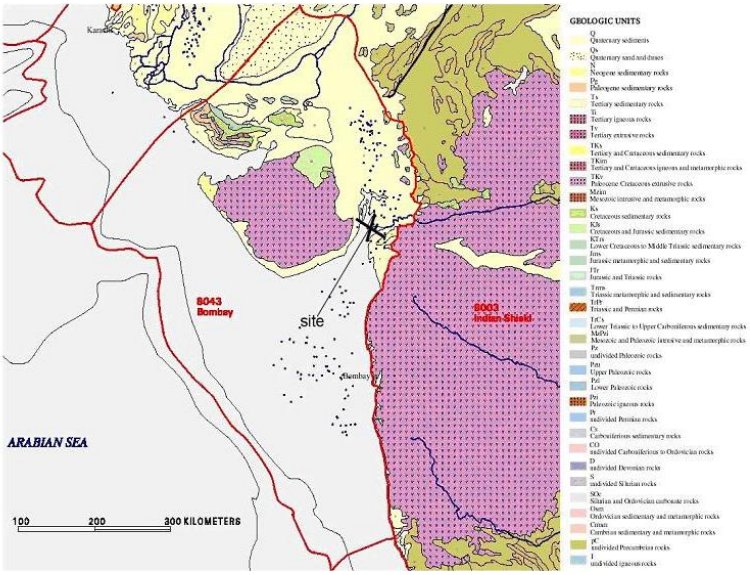

Figure 1. Geology of the region

Within the basaltic lava flows, numerous sedimentary beds of carbonates occur in Gujarat. Usually the middle part of the trap is devoid of these intertrappean beds. It is believed that the Deccan Trap is the result of sub-aerial volcanic activity associated with continental divergence during the Mesozoic.

3 Seismic information

From the viewpoint of seismic background, no single source of seismic data appeared to be sufficiently complete. Following a thorough search of the available information, three different databases were combined:

– The catalogue of the International Seismicity Centre (ISC) which covers the period from 1964 to 1998. The ISC has also a historical catalogue for the earlier years, back to 1904.

– The catalogue of the National Earthquake Information Centre of the United States Geological Survey (USGS/NEIC) with events from 1973 onwards, including very recent events.

– The historical catalogue of Rao and Rao (1984) which contains data from 1340 to 1983 of the Indian Peninsula.

For events after 1998, the USGS/NEIC catalogue was used. For the period between 1973 and 1998, events were taken from the ISC catalogue, which has data of excellent quality. Both the ISC and the Rao and Rao (1984) catalogues were taken into account for the years between 1904 and 1973. Finally, Rao and Rao (1984) provided the only information available prior to 1904. The events with magnitude $M_w > 3$ appear in Figure 2.

The seismic hazard was evaluated using the zoneless method proposed by Woo (1995, 1996a). The numerical implementation is that embodied in the computer program KERFRACT (Woo, 1996b). The basic starting data are the catalogue of past epicentres and their corresponding magnitudes, together with the knowledge of the effective period of observation for each earthquake. This allows constructing an activity rate for each location and event magnitude; the details are given in the referenced literature.

The design motions were adopted following NFPA 59A (NFPA, 1996). For evaluating the seismic hazard, the attenuation relation developed by Boore et al (1997) was adopted, using suitable parameters. Figure 3 shows this attenuation law for period T = 0 s and a soil site and Figure 4 for period T = 0.2 s and again a soil site. In both cases it has been plotted for various values of the moment magnitude (M_w) of the earthquake.

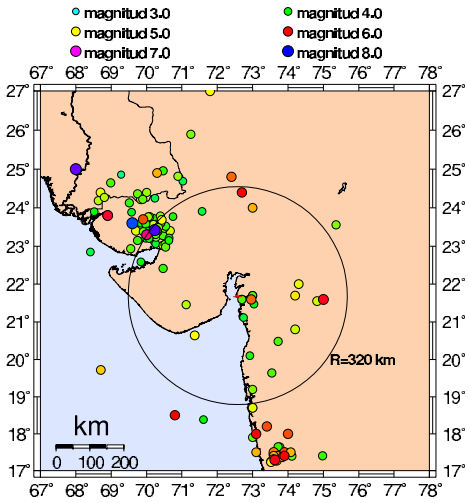

Figure 2. Epicentres considered with magnitudes M_w above 3.0

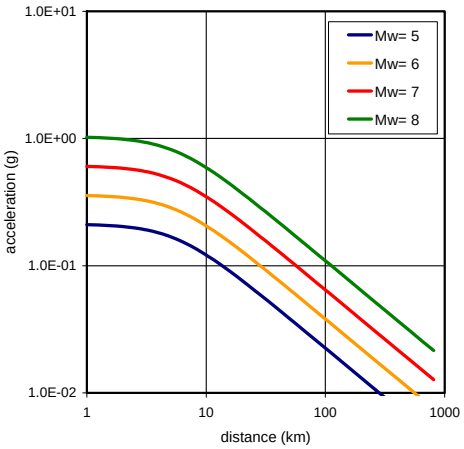

Figure 3. Attenuation for T = 0 s, soil site (Boore et al, 1997)

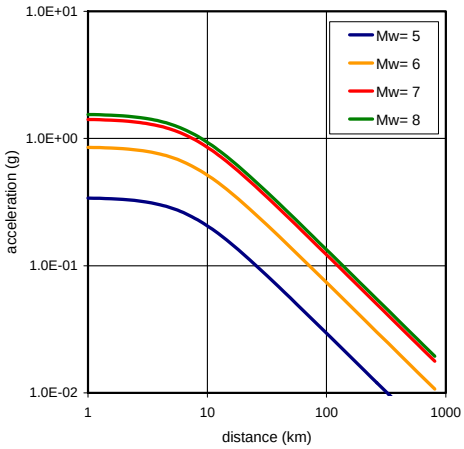

Figure 4. Attenuation for T = 0.2 s, soil site (Boore et al, 1997)

The Bhuj earthquake, which occurred on 26 January 2001, provided a benchmark for verifying the attenuation relationship. Its isoseismal map, as reported by Narula and Chaubey (2001) is presented in Figure 5. For verifying the attenuation relationship, epicentral intensities must be converted into accelerations, for which the Gutenberg and Richter (1956) correlation was used. Taking the attenuation in the direction of the Dahej site and plotting it against the Boore et al (1997) relationship for M_w= 8.2, Figure 6 indicates that the predictions match very well the observations. For comparison, the attenuation law for M_s = 8.0 derived by Ambraseys (1995) for European earthquakes, which is also shown in that figure, can be seen to predict excessive attenuations at large distances from the epicenter. The two measures of the earthquake, M_s = 8.0 and M_w = 8.2, are consistent with each other. As a consequence of all this, the attenuation proposed by Boore et al (1997) was adopted.

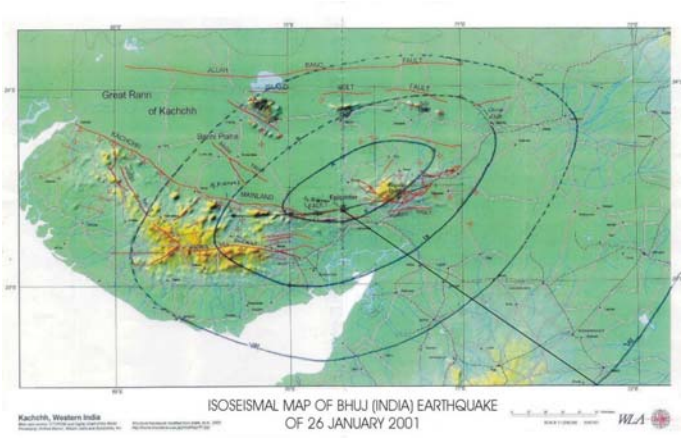

Figure 5. Isoseismal map of the 26th January 2001 earthquake in Bhuj

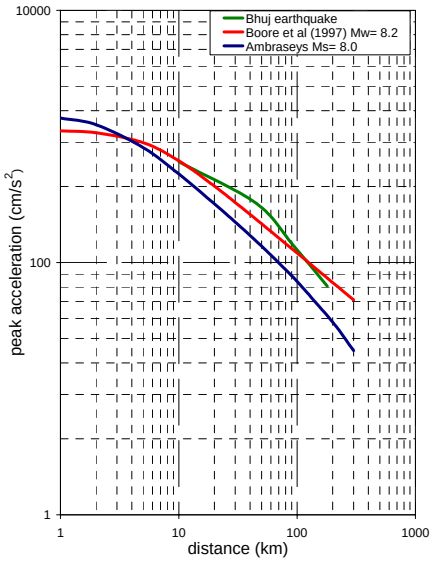

Figure 6. Attenuation of the Bhuj earthquake and some attenuation models

Hazard curves, relating the accelerations to the different probabilities of occurrence, are shown in Figure 7: one corresponds to the peak ground acceleration (PGA), a second one provides accelerations for T = 0.2 s and the third and fourth ones those for T = 1 s and T = 2 s. The periods selected are the relevant ones for defining the design spectra following the ASCE 7-02 (ASCE, 2003).

By obtaining the acceleration values for other periods of vibration, uniform hazard spectra can be constructed for the return periods of interest. Figure 8 shows six such spectra, which correspond to return periods of 100, 475, 1000, 2475, 5,000 and 10,000 years. Table 2 presents some of the results.

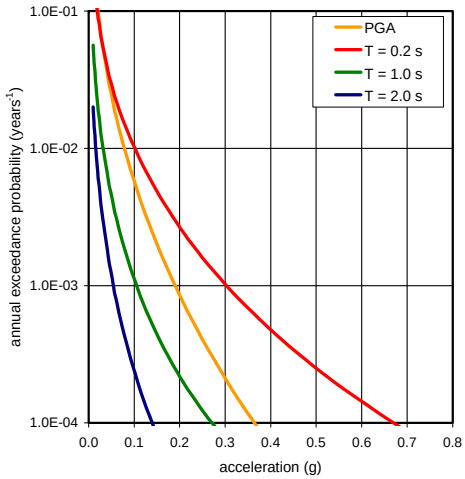

Figure 7. Seismic hazard curves for PGA, T = 0.2 s, T = 1.0 s and T = 2.0 s

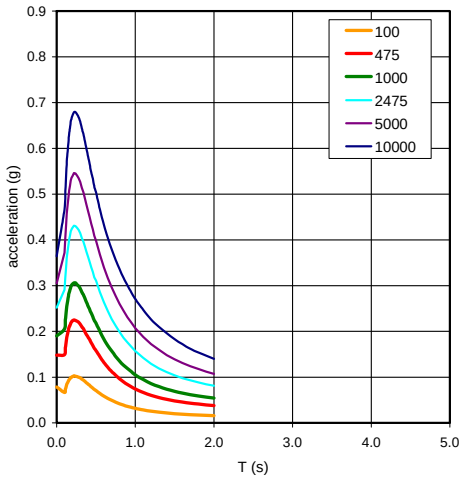

Figure 8. Uniform hazard spectra for several return periods

Table 2. Accelerations in g's for relevant return periods and spectral periods

Return period	PGA	T = 0,2 s	T = 1 s	T = 2 s
475 (OBE)	0.148	0.223	0.074	0.038
2,475	0.252	0.426	0.157	0.081
5,000	0.305	0.539	0.207	0.107
10,000 (SSE)	0.364	0.671	0.271	0.140

The design motions adopted are very conservative, as later revisions of NFPA 59A have led to a return period for the SSE four times shorter than that used here. As a matter of interest the new tanks T-103 and T-104, designed after the norm had changed, kept the same design motions in spite of the fact that it was no longer necessary, an indication of the safety conscious orientation of the design specifications.

4 Foundation design

The foundation of each one of the two tanks is made of 578 piles, 1 m in diameter and about 36 m long (including 2 m above the surface); the precise length depends on the specific depth at which the dense sands are found at each location. The piles are cast-in-situ, reinforced concrete piles, with their pileheads rigidly connected to a 1 m thick base slab, elevated 2 m above the ground surface. The configuration can be seen in Figure 9.

The loads and load combinations that the tanks and their foundations must face, as well as the success criteria to be used in the evaluation of the response, were laid out in the Design Criteria developed at the beginning of the project. Pile demands were calculated under the various load combinations and peak demands were established for SLS and ULS conditions for test, normal and abnormal loads.

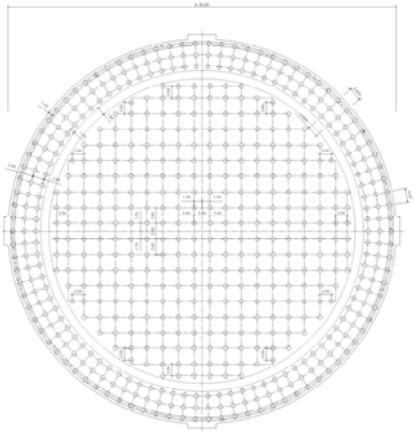

Figure 9. Plan view of the pile configuration

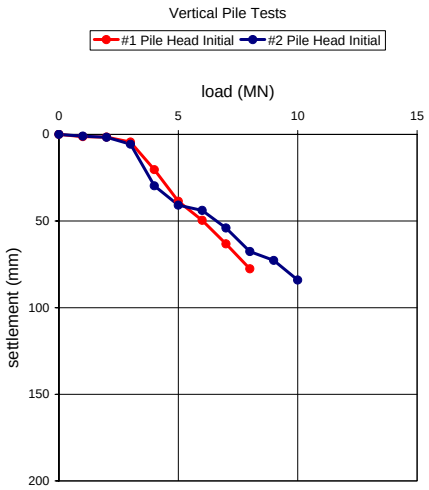

Figure 10. Results of the axial pile tests

4.1 Axial loads

The maximum axial demands expected are given in Table 3. The estimated pile capacity, using conventional approaches, was considerably greater than the expected axial demands.

Table 3. Peak axial demands

	SLS	ULS
Minimum axial force (MN)	0.26	-0.20
Maximum axial force (MN)	3.48	4.64

Two valid tests were conducted; there was a third one in which the pile was too short. The piles were 36 m long and entered 4-5 m into the dense sand. The results obtained in the tests are shown in Figure 10. Reasonable extrapolations suggest "safe loads" (half of those inducing settlements of 10% of the diameter) of 4.75 and 5.75

MN, averaging 5.25 MN: this is much higher than the SLS demands (3.48 MN). The seismic capacity, being 50% greater, is 7.88 MN, again much higher than the ULS demands (4.64 MN).

4.2 Horizontal loads

Horizontal movements of the pile heads cause shear forces and bending moments in the piles. The peak horizontal demands appear in Table 4, together with the minimum values of the associated axial compression.

Table 4. Peak shear demands

	SLS	ULS
Horizontal load (MN)	0.55	1.03
Minimum axial (MN)	1.48	1.51

The shear capacity of the piles is a function of the axial load applied. The piles have four different sections, depending on the reinforcement configuration; the upper one is broken into two subsections as a consequence of the reduction of seismic origin experienced in the upper 1 m (formation of the hinge). As an example Figure 11 shows the distribution of shear demands along a pile, together with the capacities at each depth.

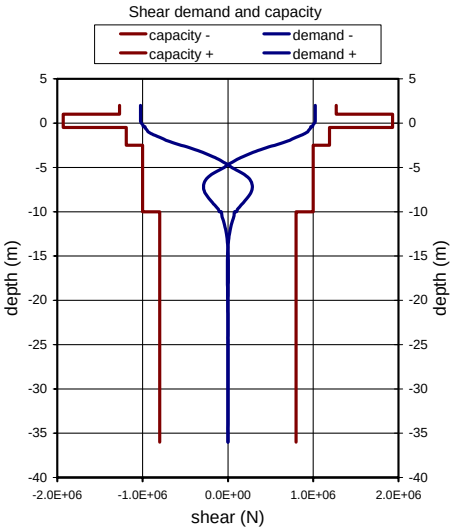

Figure 11. Shear demands and capacity with depth

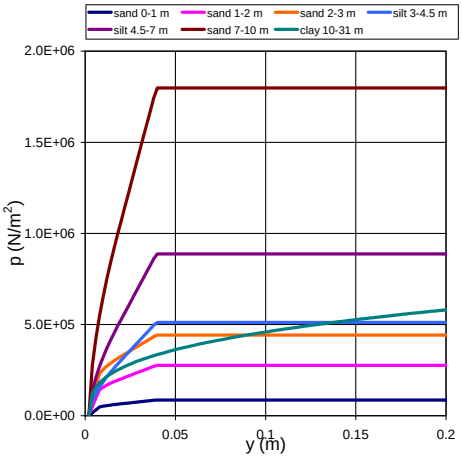

Figure 12. *p-y* curves at the various depths

The peak moments developed under the various load combinations were also taken into account. The maximum values are given in Table 5. Two values appear under ULS conditions; although the second one has a lower demand, its capacity is also smaller because of lower axial compression.

Table 5. Peak moment demands

	SLS	ULS_1	ULS_2
Peak moment (MNm)	2.34	4.37	4.12
Minimum axial load (MN)	2.67	3.09	1.51

Several differences exist between the piles used in the foundation and those tested in the field. The main one is that foundation piles have rotations constrained by the slab, which leads to the peak moments being developed at the pile head. By contrast, an isolated pile is free to rotate and has zero moments at the pile head; the peak moments occur at some depth below the surface. This causes differences in response between the two piles; moreover, as the reinforcement is designed for the foundation piles, its configuration is far from optimal for the demands experienced by test piles. Hence, lateral capacities obtained in tests might not be directly usable for foundation piles. In order to deal with this problem the approach followed consisted in calculating the expected responses of both test and foundation piles. The former could be confirmed by testing; as the latter used identical methodology, confirmation of the former could be taken also as confirmation of the latter.

The calculations were based on a beam model of the pile, characterised in each region by the corresponding moment-curvature relationship, and by non-linear *p-y* curves describing the interaction of the pile with the soil at each depth. The curves were developed following the methodology of Maymand and Lok (1999) and are shown in Figure 12 for the various depth ranges of interest.

The capacity of the piles in bending was studied both when the pile is part of the tank foundation and for a single pile. Figure 13 shows the expected force-displacement behaviour of the pile in its final configuration in the foundation; similarly, Figure 14 presents similar information in terms of the moment at the pilehead; the allowable limits are shown under OBE and SSE conditions. As can be seen, the available capacities are in principle sufficient to carry the bending demands imposed.

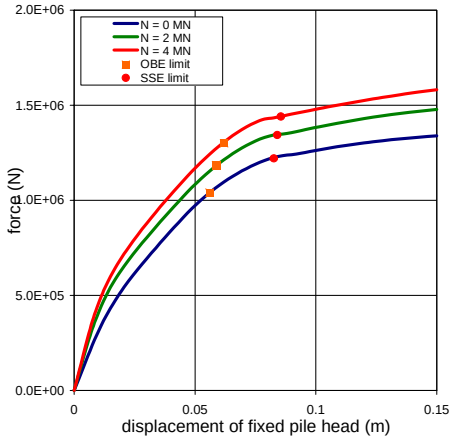

Figure 13. Pile capacity in bending: force-displacement

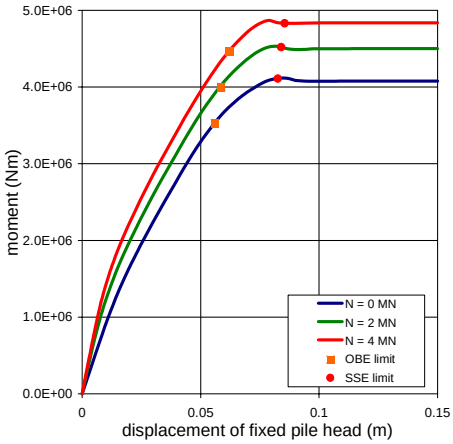

Figure 14. Pile capacity in bending: moment- displacement

The distributions of the bending demands along the pile are presented in Figures 15 for an axial compression of 1.51 MN; the available capacities at each depth have also been plotted for comparison. Again, capacities are sufficient for carrying the demands.

In the two field tests conducted with lateral loads on individual piles, a horizontal load of 0.6 MN was applied with an almost linear response of the pile-soil assembly (Figure 16). This is in spite of the fact that the reinforcement configurations are not adequate for the test pile with a free pilehead. The figure shows the experimentally obtained curves, up to 0.6 MN, together with the pre-test analytical predictions of the behaviour under lateral loads; the analytical prediction also shows the points where the acceptability limits would be exceeded with OBE and SSE criteria. The methodology adopted is therefore reasonably accurate and conservative.

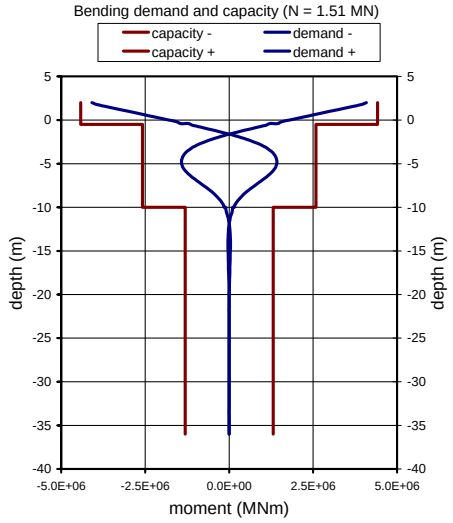

Figure 15. Bending demand and capacity with depth (N = 1.51 MN)

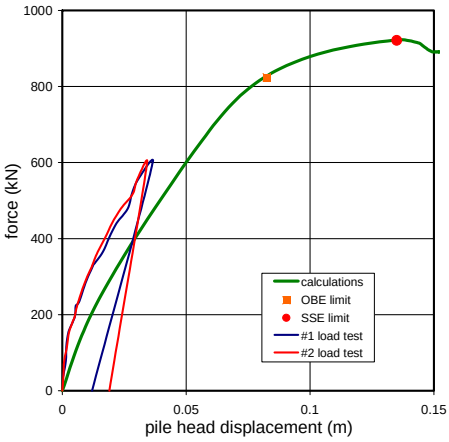

Figure 16. Predicted and measured lateral load tests

5 Conclusions

Out of the work conducted for designing the first two LNG storage tanks at Dahej (Gujarat), the paper has concentrated on the seismic environment and its implications on the pile foundations of the tanks. Some conclusions can be offered as a result of this work:

a) The seismic motions used for design are very conservative, particularly in respect of the SSE. A return period of 10,000 years was used for that earthquake while current norms contemplate periods in the region of 2,475 years in USA to 4.975 years in Europe.

b) Even for these conservative demands, the foundation piles provide considerable margins, in respect of both vertical and horizontal loads.

c) The expected axial performance of the piles can be directly confirmed in field tests, as was successfully done following the provisions of IS 2911.

d) The performance under horizontal loads cannot be tested directly because the pile head is free to rotate in a test pile but not in a foundation pile. By calculating both of types of behaviour and confirming the expectations for the case of the test pile, adequate confidence could be also placed on the expectations for foundation piles.

6 References

Ambraseys, N.N. (1995) “The Prediction of Earthquake Peak Ground Acceleration in Europe”, Earthquake Engineering and Structural Dynamics, Vol. 24, pp. 467-490.

ASCE - American Society of Civil Engineers (2003) “ASCE 7-02. Minimum Design Loads for Buildings and Other Structures”, Second Edition.

Boore, M.B., Joyner, W.B. and Fumal, T.E. (1997) "Equations for Estimating Horizontal Response Spectra and Peak Acceleration from Western North American Earthquakes", Research Letters, Bulletin of the Seismological Society of America, Vol. 68, no. 1.

Gutenberg, B. and Richter, C.F. (1956) “Earthquake Magnitude, Intensity, Energy and Acceleration”, Bulletin of the Seismological Society of America, Vol. 32, No. 3, pp. 163-191.

Meymand, P.J. and Lok, T.M. (1999) “Seismic Response of Piles Research Project”, Department of Civil and Environmental Engineering, University of California, Berkeley, April.

Narula P.L. and Chaubey, S.K. (2001) “Macroseismic Surveys for the Bhuj (India) Earthquake of 26 January 2001” http://www.nicee.org/NICEE/Gujarat/narula. htm.

NFPA – National Fire Protection Association (1996) “NFPA 59A. Standard for the Production, Storage and Handling of Liquefied Natural Gas, 1996 Edition”.

Rao, B.R. and Rao, P.S. (1984) "Historical Seismicity of Peninsular India", Bulletin of the Seismological Society of America, Vol. 74, No. 6, April, pp. 353-362.

Woo, G. (1995) “A Comparative Assessment of Zoneless Models of Seismic Hazard”, 5th International Conference on Seismic Zonation, Vol. I., Nice, France, October.

Woo, G. (1996a) “Kernel Estimation Methods for Seismic Hazard Area Modelling”, Bulletin of the Seismological Society of America, Vol. 86, No. 2, April, pp. 353-362.

Woo, G. (1996b) “Seismic Hazard Program: KERFRACT”, Program Documentation.